Neutron spin structure with polarized deuterons and spectator proton tagging at EIC



2014 J. Phys.: Conf. Ser. 543 012007

(http://iopscience.iop.org/1742-6596/543/1/012007)

# Neutron spin structure with polarized deuterons and spectator proton tagging at EIC

**W Cosyn[1], V Guzey[2], D W Higinbotham[3], C Hyde[4], S Kuhn[4], P Nadel-Turonski[3], K Park[4], M Sargsian[5], M Strikman[6], C Weiss[3]**

[1] Ghent University, 9000 Gent, Belgium
[2] Petersburg Nuclear Physics Institute, Gatchina, 188300, Russia
[3] Jefferson Lab, Newport News, VA 23606, USA
[4] Old Dominion University, Norfolk, VA 23529, USA
[5] Florida International University, Miami, FL 33199, USA
[6] Pennsylvania State University, University Park, PA 16802, USA

E-mail: weiss@jlab.org

**Abstract.** The neutron's deep–inelastic structure functions provide essential information for the flavor separation of the nucleon parton densities, the nucleon spin decomposition, and precision studies of QCD phenomena in the flavor–singlet and nonsinglet sectors. Traditional inclusive measurements on nuclear targets are limited by dilution from scattering on protons, Fermi motion and binding effects, final–state interactions, and nuclear shadowing at $x \ll 0.1$. An Electron–Ion Collider (EIC) would enable next–generation measurements of neutron structure with polarized deuteron beams and detection of forward–moving spectator protons over a wide range of recoil momenta ($0 < p_R <$ several 100 MeV in the nucleus rest frame). The free neutron structure functions could be obtained by extrapolating the measured recoil momentum distributions to the on-shell point. The method eliminates nuclear modifications and can be applied to polarized scattering, as well as to semi-inclusive and exclusive final states. We review the prospects for neutron structure measurements with spectator tagging at EIC, the status of R&D efforts, and the accelerator and detector requirements.

## 1. Introduction

The program of exploring short-range nucleon structure and strong interaction dynamics with high–energy lepton scattering relies on measurements on the neutron as much as those on the proton target. Neutron and proton data are needed to separate the isoscalar and isovector combinations of the deep-inelastic scattering (DIS) structure functions, which are subject to different short–distance dynamics (QCD evolution, higher–twist effects, small–$x$ behavior) and give access to different combinations of the parton densities (gluons and singlet quarks vs. non-singlet quarks). The unpolarized isovector structure function $F_{2p} - F_{2n}$ constrains the flavor composition of the nucleon's sea quark densities and permits study of small–$x$ dynamics in the non-singlet sector. In the polarized case the isovector structure function $g_{1p} - g_{1n}$ can be used to cleanly separate leading–twist and higher–twist dynamics, taking advantage of its simple QCD evolution (no mixing with gluons). The isoscalar combination $g_{1p} + g_{1n}$ can then be used to extract the polarized gluon density from the leading–twist QCD evolution. Both isospin combinations are needed to determine the flavor decomposition of the polarized quark densities and their contributions to the nucleon spin. Neutron and proton data combined are needed also to investigate the dynamical mechanism causing single–spin asymmetries in semi-inclusive DIS (where there are hints of surprisingly large isovector structures) and to constrain the generalized parton distributions in deeply–virtual Compton scattering.

Neutron structure is measured in high–energy scattering experiments with nuclear targets. The extraction of the free neutron structure functions from nuclear DIS data faces considerable challenges (see Ref. [1] for a review). Nuclear binding modifies the apparent neutron structure functions through the Fermi motion and other dynamical effects. At moderate momentum transfers $Q^2 \sim$ few $\text{GeV}^2$ the nuclear cross sections are affected by final–state interactions involving other nucleons. At $x \ll 0.1$ the large coherence length of the electromagnetic probe causes quantum–mechanical interference of the amplitudes for scattering from different nucleons along its path, which results in shadowing and antishadowing effects in the cross section [2]. In polarized measurements with light nuclei (deuteron $D \equiv {}^2\text{H}$, ${}^3\text{He}$) there is significant dilution from scattering on the proton(s). One must know not only the degree of neutron polarization in the nucleus but also the spin dependence of the various nuclear modifications of nucleon structure. Attempts to account for these nuclear effects theoretically are complicated by the fact that they arise as an average over different classes of configurations in the nuclear wave function, which cannot be separated in inclusive measurements. It is clear that better experimental control of the nuclear environment is needed to improve the precision of neutron structure extraction. This is particularly relevant if a combination of neutron and proton data are to be used to study subtle QCD effects, such as the separation of leading and higher twist, non-singlet QCD evolution, and non-singlet small–$x$ behavior.

Inclusive deep–inelastic scattering from nuclei was measured in fixed–target experiments with electron and muon beams, at electron–nucleon squared center–of–mass energies $s_{eN} \equiv s_{eA}/A$ in the range $s_{eN} \sim 10 - 900\,\text{GeV}^2$ (JLab 6 GeV, DESY HERMES, SLAC, CERN EMC/NMC, FNAL E665; see Refs. [1, 3] for a review of the data). Measurements of neutron spin structure with polarized nuclear targets were performed at SLAC, DESY HERMES, CERN SMC/COMPASS and JLab 6 GeV [4, 5, 6]. Both unpolarized and polarized nuclear measurements will be extended with the JLab 12 GeV Upgrade [3]. While these experiments have provided basic information on neutron structure at $x \gtrsim 0.01$, addressing the above questions will require data of much higher precision and wider kinematic coverage.

The Electron–Ion Collider (EIC), proposed as a next-generation facility for nuclear physics, would dramatically expand the opportunities for high-energy scattering on polarized light nuclei ($D$, ${}^3\text{He}$, $\ldots$) and measurements of neutron structure.[1] The medium–energy EIC designs recently developed provide electron–nucleon squared center–of–mass energies in the range $s_{eN} \sim 250 - 2500\,\text{GeV}^2$ at luminosities up to $\sim 10^{34}\,\text{cm}^{-2}\,\text{s}^{-1}$ [8]. The wide kinematic coverage would permit definitive studies of the $Q^2$ evolution and small–$x$ behavior of structure functions; the high luminosity would enable measurements of spin asymmetries and rare processes involving exceptional configurations. Even more important, two specific capabilities provided by the EIC would allow one to control the nuclear modifications and extract neutron structure with unprecedented precision.

One capability are deuteron beams, especially polarized deuterons, as would be available for the first time with the JLab MEIC, thanks to the figure–8 shape of the ion ring designed to compensate the effect of spin precession [9]. The deuteron is the simplest nucleus ($A = 2$); its wave function is known well up to large nucleon momenta $\sim 300$ MeV, including the light-front wave function describing microscopic nuclear structure as probed in high-energy scattering processes [10]. The deuteron has spin 1 and is mostly in the $L = 0$ configuration (S–wave), with a small admixture of $L = 2$ (D–wave), such that the proton and neutron are spin–polarized and their degree of polarization is known very well. Because there are only two nucleons the

[1] For a general overview of the medium–energy EIC physics program, including measurements with proton beams, see e.g. Ref. [7].

possibilities for final–state interactions are limited; in the configurations where they can happen they can be estimated using theoretical models (see e.g. Refs. [11, 12] for a model in the resonance region $W \sim$ few GeV).

The other capability is the detection of spectator nucleons emerging from the high–energy scattering process ("spectator tagging"). In collider experiments the spectator nucleons carry a fraction $\sim 1/A$ of the ion beam momentum and can be detected with appropriate forward detectors. The technique is uniquely suited to colliders: there is no target material absorbing low-momentum nucleons, and it can be used with polarized ion beams (longitudinal and transverse). Spectator tagging is especially powerful in scattering on the deuteron. It allows one to positively identify the active neutron through proton tagging, and to control its quantum state through measurement of the recoil momentum. Spectator proton tagging with unpolarized deuterium was explored in a pioneering fixed-target experiment at JLab with 6 GeV beam energy (CLAS BoNuS detector, covers recoil momenta $p_R \gtrsim 70\,\text{MeV}$) [13] and will be studied further at 11 GeV.

In this note we summarize the potential of DIS on the deuteron with spectator proton tagging for precision measurements of the neutron structure functions at EIC. We describe the method for eliminating nuclear structure effects through on-shell extrapolation in the spectator proton momentum, present simulations of unpolarized and polarized observables [14], and outline the accelerator and detector requirements. It should be noted that the various nuclear modifications of the nucleon's partonic structure are interesting physics topics in their own right (with connections to short-range $NN$ correlations, non-nucleonic degrees of freedom, etc.) and can be studied with the same spectator tagging measurements at larger recoil momenta [15].

## 2. Neutron structure with spectator tagging

The basic method for extracting the free neutron structure function with spectator tagging is described in Ref. [16] (see Fig. 1). One measures the cross section of conditional DIS $e + D \to e' + p + X$ as a function of the recoil proton momentum, parametrized by the light–cone fraction $\alpha_R \equiv 2(E_R + p_R^z)/(E_D + p_D^z)$ and the transverse momentum $\boldsymbol{p}_{RT}$, defined in a frame where the deuteron momentum $\boldsymbol{p}_D$ and the $\boldsymbol{q}$ vector are collinear and along the $z$–direction (see Fig. 1a). A key variable is the invariant 4–momentum transfer between the deuteron and the recoil proton, $t \equiv (p_R - p_D)^2$, calculated from $\alpha_R$ and $\boldsymbol{p}_{RT}$. As a function of $t$ the scattering amplitude has a pole at $t = M_N^2$, which arises from the impulse approximation diagram of Fig. 1b and corresponds to "neutron exchange" in the $t$–channel. The residue at the pole is, up to a constant factor representing deuteron structure, given by the structure function of the *free neutron,* evaluated at the argument $\tilde{x} = x/(2 - \alpha_R)$, where $x = Q^2/(p_D q)$ is the scaling variable with $0 < x < 2$. [2] It can be shown that nuclear binding and final–state interactions only affect the amplitude at $M_N^2 - t > 0$, but not the residue at the pole [16].

To extract the free neutron structure function one plots the measured tagged cross section as a function of $t$, removes the pole factor $1/(M_N^2 - t)^2$, and extrapolates to $t \to M_N^2$ [16]. The pole in $t$ is extremely close to the physical region, so that the extrapolation can be performed with great accuracy; the minimum physical value of $M_N^2 - t$ is $\epsilon_D M_D$, where $\epsilon_D$ is the deuteron binding energy. The method is analogous to the Chew–Low extrapolation used to extract pion structure from $\pi N$ scattering data. Figure 1c shows a simulated on-shell extrapolation with MEIC pseudodata ($s_{eN} = 1000\,\text{GeV}^2$, integrated luminosity $10^6\,\text{nb}^{-1}$) [14]. One sees that the $t$–dependence is very smooth. The extrapolation in $t$ is performed at *fixed* values of the recoil light-cone fraction $\alpha_R$, such that the effective $\tilde{x}$ in the neutron structure function remains constant along the way. Figure 1c shows the pseudodata in three bins of $\alpha_R$ with average values $\langle \alpha_R \rangle = (1,\ 1.04,\ 1.08)$ and a width of 0.04. Note that the kinematic limit in $M_N^2 - t$ increases

[2] The variables are defined such that in the absence of nuclear binding $\alpha_R = 1$, and $x = \tilde{x}$ coincides with the usual scaling variable for scattering from a free nucleon.

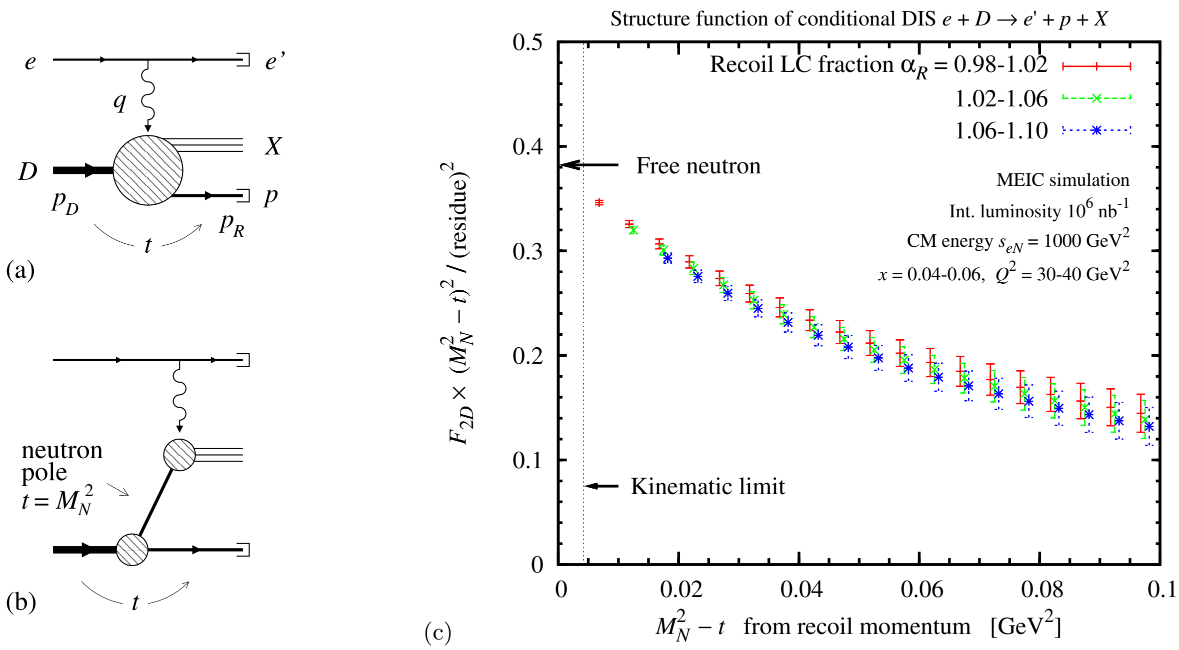


**Figure 1.** (a) Conditional DIS on the deuteron, $e + D \to e' + p + X$. (b) Neutron pole at $t = M_N^2$ arising from the impulse approximation diagram. (c) Simulated measurement of the recoil momentum dependence with MEIC and on-shell extrapolation $t \to M_N^2$ [14]. The plot shows the conditional structure function, with the pole factor $1/(M_N^2 - t)^2$ and the residue removed, as a function of the off-shellness $M_N^2 - t$ calculated from the measured proton recoil momentum. The error bars indicate the expected statistical errors. The three sets correspond to measurements in different intervals of the recoil light–cone momentum fraction $\alpha_R$.

from $\epsilon_D M_D$ as $\alpha_R$ moves away from unity. Comparison of the extrapolation results at different $\alpha_R$ allows one to confirm the universality of the nucleon pole and provided an important test of the theoretical framework. Critical to the success of the method is the ability to measure the recoil proton momentum with complete coverage down to $p_{RT} = 0$, and with a resolution $\Delta p_{\mathrm{RT}} \lesssim 20\,\mathrm{MeV}$ and $\Delta\alpha_R \lesssim 10^{-3}$.

The method described here permits a clean and model-independent extraction of free neutron structure and would enable precision measurements of $F_{2n}$ over the entire $x$–$Q^2$ range accessible with EIC. Combined with proton data taken in the same kinematics it would determine the isovector structure function $F_{2p} - F_{2n}$, which constrains the flavor structure of the nucleon sea. The results could be cross–checked against those from dilepton production in $pp/\bar{p}p$ collisions, which separate quark flavors through selection of $\gamma^*$ (Drell–Yan), $Z$, and $W^\pm$ events, and be used to test the universality of the sea quark densities [17]. The isovector $F_{2p} - F_{2n}$ would also permit quantitative studies of small–$x$ dynamics in the non-singlet sector, which is largely unexplored and raises many interesting questions (QCD structure of Reggeon exchange, non-singlet diffraction, etc.). In practice such studies will likely be limited to the region $x > 0.01$, as the difference between proton and neutron structure functions becomes very small at low $x$ $[(F_{2p} - F_{2n})/(F_{2p} + F_{2n}) < 0.02$ at $x < 0.01$ for $Q^2 \sim$ several 10 GeV$^2$] and would be increasingly difficult to determine from separate measurements. Lastly, the results for $F_{2n}$ itself would serve as stringent test for models of nuclear effects in heavier nuclei.

DIS on the deuteron with spectator proton tagging could be used to address other interesting physics questions besides free neutron structure. The recoil momentum dependence of the effective neutron structure function in $e + D \to e' + p + X$ allows one to study the modification of the neutron's partonic structure as a function of its momentum in the deuteron wave function — a qualitative improvement compared to usual inclusive measurements. Theoretical arguments suggest that the modification of the effective neutron structure function in the deuteron is in first approximation proportional to the neutron's virtuality $M_N^2 - t \approx 2|\boldsymbol{p}_R|^2$(rest frame), which is controlled by the measured recoil momentum [18]. Furthermore, the modification is related in a simple way to the EMC effect in inclusive nuclear structure functions of heavier nuclei ($A > 2$) and exhibits similar $x$–dependence. Measurements of the recoil momentum dependence of the effective neutron structure function in $e + D \to e' + p + X$ thus provide direct insight into the dynamical origin of the EMC effect. In particular, measurements at large recoil momenta $|\boldsymbol{p}_R|$(rest frame) $\gg 100\,\text{MeV}$ could verify a possible connection between the EMC effect and short–range $NN$ correlations in nuclei [19, 20].

Measurements of the recoil momentum dependence in $e + D \to e' + p + X$ at finite $|\boldsymbol{p}_{RT}|$ and $\alpha_R \neq 1$ also provide a unique method for studying nuclear final–state interactions in DIS at $Q^2 \sim$ few $\text{GeV}^2$. The results of such measurements could be used to refine phenomenological models of the final–state interactions [11, 12], which would improve the precision of neutron structure extraction from inclusive nuclear scattering data (including $A > 2$).

## 3. Neutron spin structure

Polarized DIS on the deuteron with spectator proton tagging can be used to determine the free neutron spin structure function $g_{1n}$. The method for eliminating nuclear effects described above can straightforwardly be extended to double–polarized scattering. The simplest case is that of a longitudinally polarized electron beam colliding with a longitudinally polarized deuteron beam, where "longitudinal" refers to the respective beam directions.[3] One measures the cross section of conditional double–polarized DIS $\vec{e} + \vec{D} \to e' + p + X$ as a function of the recoil proton momentum variables; the recoil proton polarization remains undetected and is summed over. The on-shell extrapolation in $t$ could in principle be performed directly with the polarized cross sections, using the same formulas as in the unpolarized case. It is more convenient, however, to work with the spin asymmetry

$$A_{\parallel} = \frac{\sigma(++) - \sigma(+-)}{\sigma(++) + \sigma(+-)}, \tag{1}$$

where $\sigma(\lambda_e, \lambda_D)$ denotes the conditional cross section for the spin projections $\lambda_e = \pm 1/2$ and $\lambda_D = \pm 1$. In Eq. (1) the nucleon pole $1/(M_N^2 - t)^2$ in the cross sections cancels between numerator and denominator (as do most of the nuclear modifications at $M_N^2 - t > 0$), and the asymmetry naturally has a smooth dependence on $t$. Figure 2 shows a simulated measurement of the conditional spin asymmetry at MEIC as a function of $t$ ($s_{eN} = 1000\,\text{GeV}^2$, integrated luminosity $2 \times 10^7\,\text{nb}^{-1} = 20$ times higher than in the unpolarized simulation of Fig. 1c) [14]. The projections shown here were made using a simple model of deuteron structure that does not include the $D$–wave, assumes the same nuclear modification of polarized and unpolarized cross sections at $M_N^2 - t > 0$, and therefore does not have an explicit $t$–dependence of the asymmetry; in a more realistic model there would be a weak residual $t$–dependence at $M_N^2 - t > 0$ due to the said effects. Figure 2 shows that an accurate measurement of the conditional spin asymmetry could be made over a range of $M_N^2 - t \lesssim 0.05\,\text{GeV}^2$ with the proposed setup, and that the on-shell extrapolation could be performed as in the unpolarized case. More elaborate simulations, assuming general deuteron polarization (mixed states, tensor polarization) and using realistic deuteron wave functions, are in progress [14].

[3] In the present MEIC design the electron and deuteron beam collide with a finite crossing angle $\sim 50\,\text{mrad}$; its effect on the net polarization along the $\boldsymbol{q}$ vector direction can easily be calculated and is very small.

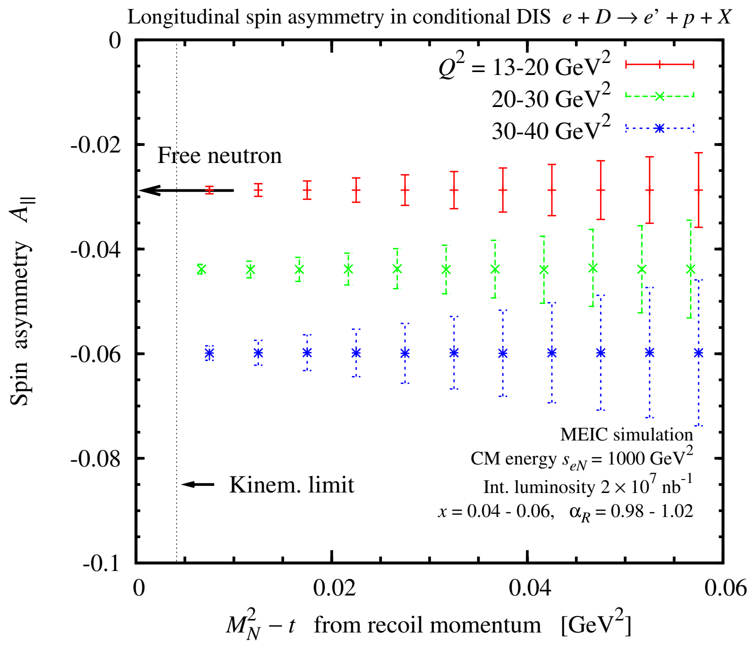


**Figure 2.** Simulated measurement of the longitudinal double spin asymmetry $A_{\parallel}$, Eq. (1), in conditional DIS on the deuteron with spectator proton tagging, $\vec{e}+\vec{D} \rightarrow e' + p + X$ with MEIC. The measured asymmetry is shown as a function of the off–shellness $M_N^2 - t$, calculated from the measured proton recoil momentum, in a single interval of the recoil light-cone momentum fraction $\alpha_R$. The error bars indicate the expected statistical errors. The three sets correspond to different values of $Q^2$.

The on-shell (extrapolated) asymmetry can then directly be used to extract the *free neutron* spin structure function. An important simplification occurs because the $D$–wave contribution to the cross section is very small at the on-shell point, as it is proportional to a higher power of the recoil proton rest–frame momentum. It implies that the deuteron wave function at the pole can be regarded as a practically pure $S$–wave, in which the neutron is completely polarized along the deuteron spin direction, and renders further analysis as simple as in the case of a polarized nucleon target:

$$A_{\parallel}\,(\text{on-shell}) \quad \sim \quad D\, g_{1n}/F_{1n} \qquad (\text{up to terms} \sim M_N^2/Q^2), \tag{2}$$

where $D$ is a kinematic factor (depolarization factor), and the neutron structure functions are evaluated at $\tilde{x} = x/(2-\alpha_R)$ (complete expressions will be given elsewhere). Spectator tagging with on-shell extrapolation thus overcomes both the dilution and the neutron polarization uncertainties associated with inclusive nuclear measurements.

The method outlined here would enable precision measurements of the neutron spin structure function $g_{1n}$ over a wide kinematic range without any model-dependent nuclear structure input. The neutron data thus obtained could be used in several ways to advance our understanding of nucleon spin structure and QCD. Combined with the proton data they would determine the isovector polarized structure function $g_{1p} - g_{1n}$, which exhibits particularly simple QCD evolution (no mixing with gluons) and can be used to cleanly separate leading–twist and higher–twist dynamics. They would also enable precision tests of the Bjorken sum rule, and possibly a determination of the strong coupling $\alpha_s$ competitive with other methods (see Ref. [21] for a

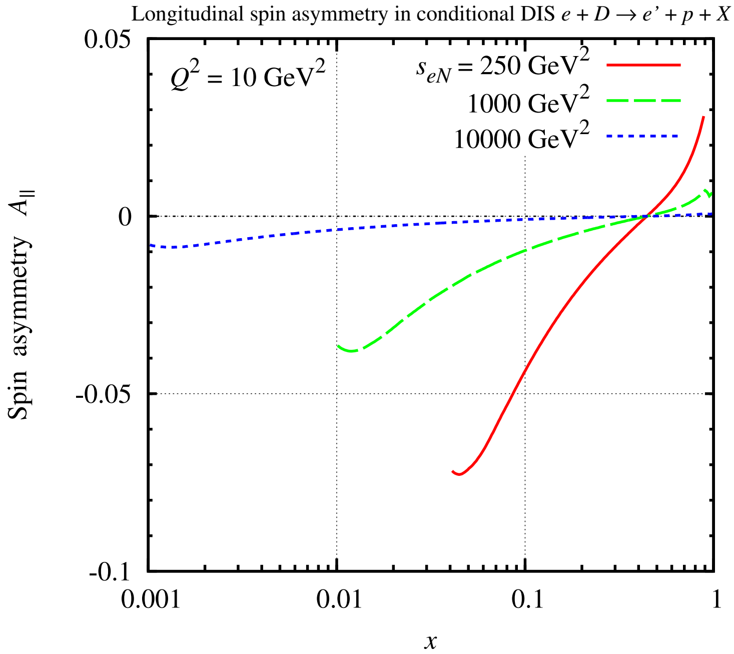


**Figure 3.** The observable double spin asymmetry $A_{\|}$, Eq. (1), in conditional DIS on the deuteron with spectator proton tagging, $\vec{e}+\vec{D} \to e'+p+X$, as a function of $x$, at $Q^2 = 10\,\text{GeV}^2$. The three curves correspond to measurements at squared electron–nucleon center-of-mass energies $s_{eN} = 250, 1000$ and $10000\,\text{GeV}^2$. The kinematic range in $x$ available at a given energy is $x > Q^2/s_{eN}$.

recent analysis using fixed–target data). The isoscalar structure function $g_{1p} + g_{1n}$ could be used to determine the polarized gluon density from the leading–twist QCD evolution. Proton and neutron data combined would allow one to better separate quark and gluon contributions to the nucleon spin, and to determine the flavor composition of the quark spin. The status of global QCD fits to determine the polarized parton densities and the need for EIC data have have been discussed extensively in the literature. A dedicated study of the impact of spectator tagging with polarized deuterons on polarized parton densities is planned.

The center–of–mass energy of the electron–deuteron collision is an important parameter in the spin asymmetry measurements described here. According to Eq. (1) the magnitude of the observable spin asymmetry $A_{\|}$ is determined by the depolarization factor

$$D = \frac{y(2-y)}{2(1-y)(1+R)+y^2} \qquad (\text{up to terms} \sim M_N^2/Q^2), \tag{3}$$

where $R$ is the usual $L/T$ ratio of the unpolarized cross sections, and $y$ is the scaling variable measuring the electron fractional energy loss in the target rest frame. One sees that $D$ decreases proportionally to $y$ if $y \ll 1$. To maximize the observable $A_{\|}$ one wants to keep $y$ at values of order unity. Now at fixed $x$ and $Q^2$ one has $y \approx Q^2/(xs_{eN})$, where $s_{eN} \equiv s_{eD}/2$. We conclude that one should do the measurement at squared CM energies $s_{eN}$ not much larger than $Q^2/x$, such that one can keep $y$ of order unity in the region of interest. This is illustrated by Fig. 3, which shows the projected observable spin asymmetry $A_{\|}$ at a fixed $Q^2$ as a function of $x$, for different values of $s_{eN}$. The projected values of the asymmetry here were calculated using the parametrization of the neutron spin structure function provided by the global QCD fit of

Ref. [22] (the differences to more recent fits are unimportant for the point illustrated here). One sees how the observable asymmetry at a given $Q^2$ and $x$ decreases if measured at "too large" center–of–mass energies. It underscores the need for an EIC design that can deliver high luminosity over a *range of center–of–mass energies* appropriate to the measurements in question.

## 4. Semi-inclusive and exclusive measurements

The spectator tagging method described here can be extended to measurements in which the final state of the DIS process on the neutron is analyzed further in coincidence with the spectator proton. Measurements of single–inclusive hadron production in the current fragmentation region $e + D \rightarrow e' + p + h + X'$ (semi-inclusive DIS on the neutron) could further constrain the partonic structure of the nucleon by tagging the charge and flavor of the struck quark in the neutron. Combined with proton data such measurements could conclusively determine the flavor structure of the light nucleon sea (polarized and unpolarized) and separate strange and non-strange quark densities. Neutron measurements through spectator tagging could also help in exploring the dynamical mechanisms generating single–spin asymmetries in semi-inclusive hadron production (there are hints of large isovector structures, possibly related to dynamical chiral symmetry breaking) and determine the flavor structure of the nucleon's intrinsic transverse momentum distributions. Finally, spectator tagging could be used to measure exclusive processes on the neutron (deeply–virtual Compton scattering, meson production), where the isospin dependence is essential for verifying the reaction mechanism and determining the generalized parton distributions.

## 5. Accelerator and detector requirements

The spectator tagging measurements described here require integrated forward detectors with complete coverage for protons with low recoil momenta relative to beam momentum per nucleon ($p_{RT} < 200\,\mathrm{MeV}$, $p_{R\|}/p(\mathrm{beam}) \sim 0.8 - 1.2$), and sufficient recoil momentum resolution ($\Delta p_{RT} \lesssim 20\,\mathrm{MeV}$, $\Delta p_L/p_L \sim 10^{-4}$). The MEIC interaction region and forward detection system have been designed for this purpose and provide fully sufficient capabilities for the physics program outlined here [9]. The physics analysis of spectator tagging data also requires that the intrinsic momentum spread in the ion beam be sufficiently small to allow for accurate reconstruction of the actual recoil momentum at the interaction vertex. Simulations show that with the MEIC beam parameters the "smearing" of the kinematic variables is very moderate and does not substantially affect the physics analysis (the resulting uncertainty in $t$ is of the order $\sim 0.005\,\mathrm{GeV}^2$ — the bin size in Fig. 1c) [14].

The neutron spin structure measurements rely on the polarized deuteron beams that would become available with MEIC. In the figure–8 ring no significant loss of polarization is expected during acceleration and storage of either protons or deuterons, so that the polarization is essentially maintained at the source level. It is expected that a longitudinal vector polarization in excess of 70% could be achieved for a deuteron beam with $\sim 50$ GeV per nucleon [9], which would be sufficient for the measurements described here.

An R&D program in under way at JLab to develop simulation tools for spectator tagging with EIC (cross section models, event generators) and demonstrate the feasibility of such measurements [14]. The tools are being made available to users and can applied to a variety of processes of interest. Information about available resources may be obtained from the authors.

## Acknowledgments

This material is based upon work supported by the U.S. Department of Energy, Office of Science, Office of Nuclear Physics under contract DE-AC05-06OR23177. W Cosyn is supported by Research Foundation Flanders.

Notice: Authored by Jefferson Science Associates, LLC under U.S. DOE Contract No. DE-AC05-06OR23177. The U.S. Government retains a non–exclusive, paid–up, irrevocable, world–wide license to publish or reproduce this manuscript for U.S. Government purposes.

## References

[1] Arneodo M 1994 *Phys. Rept.* **240** 301
[2] Frankfurt L, Guzey V and Strikman M 2012 *Phys. Rept.* **512** 255
[3] Malace S, Gaskell D, Higinbotham D W and Cloet I 2014 *Int. J. Mod. Phys. E* **23** 1430013
[4] Kuhn S E, Chen J-P and Leader E 2009 *Prog. Part. Nucl. Phys.* **63** 1
[5] Chen J-P, Deur A, Kuhn S and Meziani Z-E 2011 *J. Phys. Conf. Ser.* **299** 012005
[6] Aidala C A, Bass S D, Hasch D and Mallot G K 2013 *Rev. Mod. Phys.* **85** 655
[7] Accardi A, Guzey V, Prokudin A and Weiss C 2012 *Eur. Phys. J. A* **48** 92
[8] For current information on the EIC machine designs, see: `https://eic.jlab.org/wiki/` (JLab) and `https://wiki.bnl.gov/eic/` (BNL).
[9] Abeyratne S *et al* 2012 *arXiv*:1209.0757
[10] Frankfurt L L and Strikman M I 1981 *Phys. Rept.* **76** 215
[11] Cosyn W, Melnitchouk W and Sargian M 2014 *Phys. Rev. C* **89** 014612
[12] Cosyn W and Sargsian 2011 *Phys. Rev. C* **84** 014601
[13] Tkachenko S *et al* 2014 *Phys. Rev. C* **89** 045206
[14] Weiss C *et al* 2014 Materials of JLab LDRD project "Physics potential of polarized light ions with EIC@JLab," available at: `https://eic.jlab.org/wiki/index.php/Forward_Tagging`
[15] Guzey V, Higinbotham D, Hyde C, Nadel-Turonski P, Park K, Sargsian M, Strikman M, and Weiss C 2014 *arXiv*:1407.3236
[16] Sargsian M and Strikman M 2006 *Phys. Lett. B* **639** 223
[17] Martin A D, Stirling W J, Thorne R S, Watt G 2009 *Eur. Phys. J. C* **63** 189
[18] Frankfurt L L and Strikman M I 1985 *Nucl. Phys. B* **250** 143
[19] Weinstein L B, Piasetzky E, Higinbotham D W, Gomez J, Hen O and Shneor R 2011 *Phys. Rev. Lett.* **106** 052301
[20] Hen O, Higinbotham D W, Miller G A, Piasetzky E and Weinstein L B 2013 *Int. J. Mod. Phys. E* **22**, 1330017
[21] Deur A *et al* 2014, *Phys. Rev. D* **90**, 012009
[22] Gluck M, Reya E, Stratmann M and Vogelsang W 2001 *Phys. Rev. D* **63** 094005